

# Mechanism of carbon microbead formation from paraffin-pitch mixtures

T. YOKONO, K. MURAKAMI, Y. SANADA

*Faculty of Engineering, Hokkaido University, Sapporo 060, Japan*

S. SHIMOKAWA, E. YAMADA

*NMR Laboratory, Faculty of Engineering, Hokkaido University, Sapporo 060, Japan*

We have proposed a model of carbon microbead formation from the mixture of coal-tar pitch and n-paraffin under mild conditions, supported by results obtained by high-temperature and high-pressure  $^1\text{H}$  nuclear magnetic resonance and electron spin resonance in conjunction with thermogravimetric and differential thermal analysis. The data obtained by different techniques are in good agreement with each other.

## 1. Introduction

The applications of carbon materials vary widely from space, biology and electronic engineering to fine chemistry. Such carbon materials must have new and novel properties. Carbon fibre and intercalation compounds, for instance, were two of these new carbon materials. In order to produce advanced carbon materials, innovative or improved production methods are necessary. Carbon microbeads have been recognized as one of the promising carbonaceous materials for producing high density, high strength isotropic carbon solids for production of nuclear graphite [1, 2] and as a bulking agent for liquid chromatography [3].

Inagaki *et al.* [4, 5] obtained carbon microbeads from various combinations of polymers such as between polyethylene, polypropylene or polystyrene and either polyvinylchloride or polyvinylidenechloride under high-temperature and high-pressure conditions in a sealed gold tube.

Recently, we have succeeded in obtaining uniform carbon microbeads by carbonization of a mixture having the different chemical nature of n-paraffin with pitch under mild pressure and temperature conditions [6, 7]. The carbon microbeads thus obtained are expected to possess different properties from those obtained by separation from the pitch matrix.

This paper describes the mechanism of formation of carbon microbeads with the application of various analytical tools. Data were obtained from high-temperature and high-pressure  $^1\text{H}$  nuclear magnetic resonance (NMR) [8, 9], electron spin resonance (ESR) [10-12], thermogravimetry (TG) and differential thermal analysis (DTA) [13]. Special attention was focused on the co-carbonization of different groups having different carbonization characters.

## 2. Experimental procedure

### 2.1. Materials

Combinations of aromatic hydrocarbons (coal-tar pitch (CTP), 93.35% C, 4.04% H, and 1.11% N) and aliphatic hydrocarbons (n-paraffin, m.p. 341 to 343 K) were used.

All the starting materials were in powder form with particle size of 20 to 50  $\mu\text{m}$ .

### 2.2. NMR measurements

Fig. 1 shows simple NMR sample cells. One is a normal cell in which the resonance coil was wound at the bottom of the cell and the other is an upside-down cell. The purpose of orienting the cell upside down is to take NMR spectra of gases in the space above the sample. The cell is made of Pyrex glass tube. After introduction of the sample, the top of the cell was sealed. A resonance coil was wound and fixed on the cell with heat-resisting cement. The sample cell was inserted into the titanium alloy pressure vessel and nitrogen pressure of 13 MPa was applied within the vessel surrounding the sample cell.  $^1\text{H}$ -NMR spectra under high pressure were obtained in the reaction temperature range from 423 to 823 K. The spectrometer used was a Bruker SXP high-power pulse and FT spectrometer operating at 36.4 MHz.

### 2.3. ESR measurements

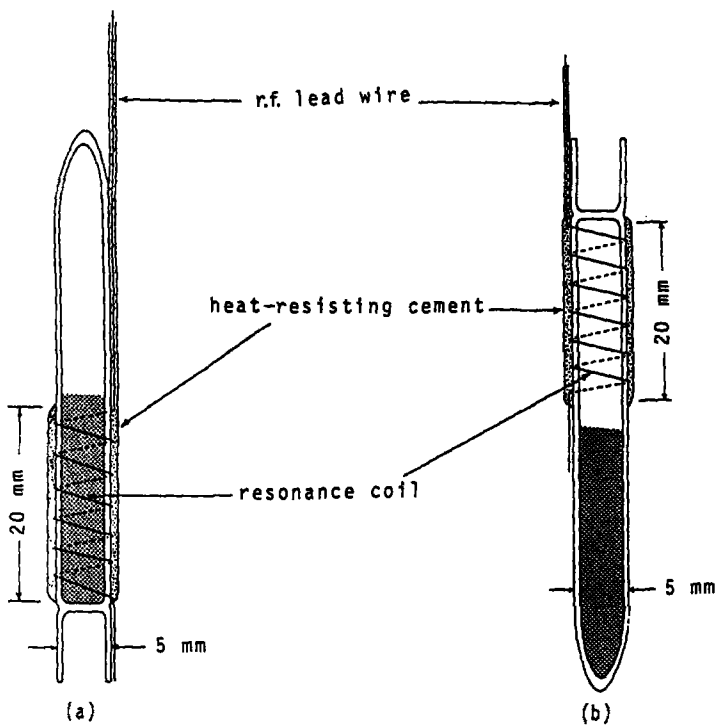
Samples were prepared in a 4 mm o.d., 1.6 mm i.d. and 15 cm long heat- and pressure-resisting quartz tube by placing the n-paraffin-pitch mixture in the bottom of the tube. The changes in spin concentration of the pitch with and without n-paraffin systems were monitored with a Varian E 109 spectrometer equipped with a cylindrical high-temperature cavity. The initial nitrogen pressure was 10 MPa. The heating rate was 5 K  $\text{min}^{-1}$ . The spectra were recorded at 7.5 sec intervals and reduced to radical concentration using a Hewlett-Packard computer.

The details of the high-temperature and high-pressure NMR and ESR cells and their operation have been published previously [8-12].

### 2.4. DTA and TG measurements

High-pressure DTA and TG were developed to enable measurement under high-temperature and high-pressure conditions [13]. The apparatus can be operated under pressures up to 13 MPa at temperatures of

Figure 1 Sample cells for NMR: (a) normal orientation, (b) upside down.



973 K. The DTA used in this study is a modified one-chamber method.

The diagram of a sample cell for TG and DTA measurement is shown in Fig. 2. The reference temperature ( $T_1$ ) in the gas reaction and the reaction temperature ( $T_2$ ) in the sample were detected, respectively. Exothermic or endothermic reactions can be detected by measuring differences in temperature between the two thermocouples and were recorded as a thermogram. A so-called "capillary open cell" was used for these TG and DTA experiments. It is bottle-shaped but with a very long narrow neck, which was not sealed during the experiment. The capillary open cell was placed on a balance which settled in the pressure vessel. The experimental pressure was 8 MPa  $N_2$ .

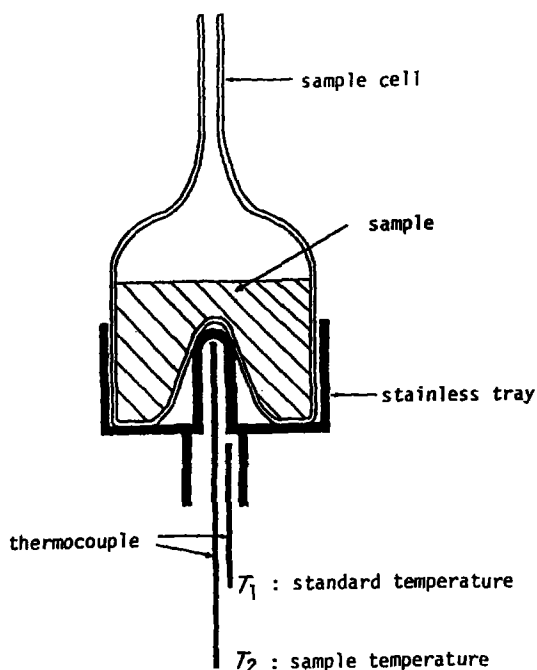


Figure 2 Diagram of sample cell for TG and DTA measurement. Differential temperature  $\Delta T = T_2 - T_1$ .

Carbonization reaction was also performed separately in a 2 ml autoclave. An autoclave charged with the sample of 0.2 g was pressurized with nitrogen at an initial pressure of 10 MPa and put into an image furnace for carbonization. Analysis of the gas evolved was carried out using flame ionization detection (FID) gas chromatography. Pure gases were used for the calibration. Scanning electron microscopy (SEM) observation was performed for the carbonization products.

### 3. Results and discussion

A typical photograph of the carbon microbeads obtained from the mixtures of n-paraffin with 20 wt % CTP is shown in Fig. 3. In order to assess the mechanism of carbon microbead formation, *in situ* measurement of high-temperature and high-pressure  $^1H$ -NMR was applied to monitor the course of the carbonization reaction for the mixtures.

Fig. 4a shows  $^1H$ -NMR spectra for the n-paraffin-CTP system using the normal NMR sample cell (Fig. 1a).

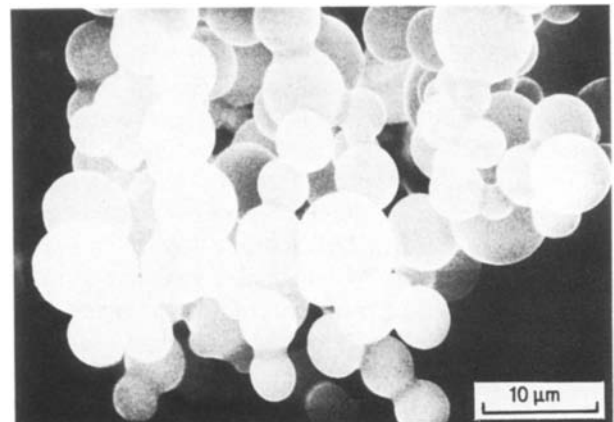


Figure 3 SEM micrograph of n-paraffin-pitch (9:1 by weight) system.

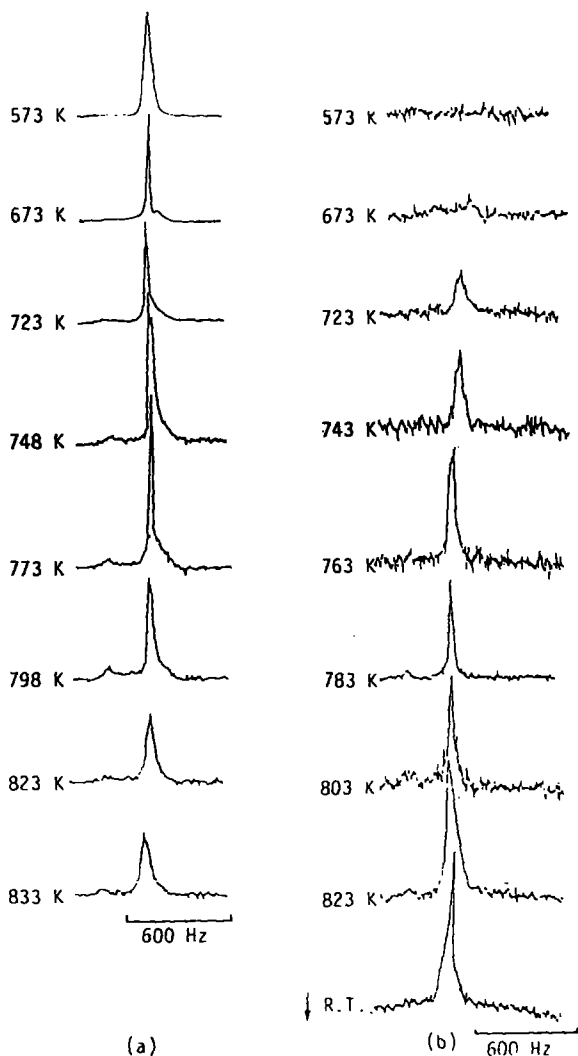


Figure 4 NMR spectra of n-paraffin-pitch system with NMR cell oriented (a) right side up (NMR coil surrounding sample), (b) upside down (NMR coil surrounding gases above sample). R.T. = room temperature.

The broad NMR spectrum for aliphatic hydrogen appears at 433 K and turns gradually sharp [6]. A new line due to aromatic hydrogen appears at a lower magnetic field at 748 K. This fact could be interpreted as follows: as a part of the n-paraffin transfers from liquid phase to gas phase and the pitch is resultantly concentrated in the liquid phase, the aromatic peak can be observed. At high temperatures, pyrolysis of n-paraffin provides rather low molecular substances in conjunction with the vaporization of n-paraffin itself, and then the aliphatic peak intensity becomes smaller\*.

NMR spectroscopy is also a very useful technique for investigating gas systems. The temperature dependence of  $^1\text{H}$ -NMR spectra for the same system but using an upside-down cell (see Fig. 1b) is shown in Fig. 4b. In this case, the appreciable NMR spectrum could be observed firstly at about 723 K. This spectrum might be due to condensed gas of n-paraffin and/or from thermal fragments of n-paraffin and pitch samples, because the NMR scan used was only 16 accumulations. With increasing temperature, the NMR signal becomes sharp. On further increase in

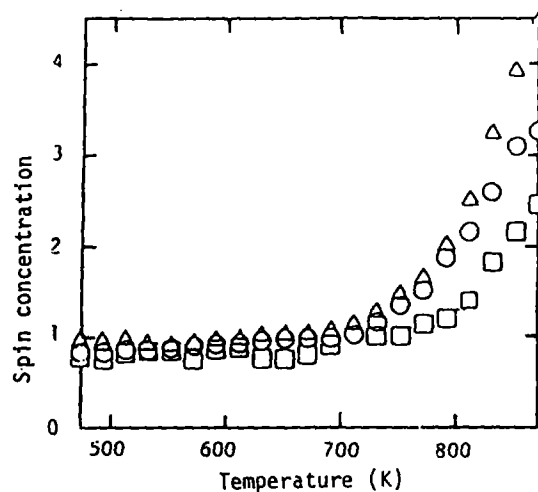


Figure 5 Temperature dependence of spin concentration (arbitrary units) of CTP with and without n-paraffin: ( $\Delta$ ) pitch alone, ( $\circ$ ) n-paraffin-pitch (1:1), ( $\square$ ) n-paraffin-pitch (9:1).  $\text{N}_2$  10 MPa,  $5 \text{ K min}^{-1}$

temperature, a new line appears at 783 K due to aromatic hydrogen. At 798 K, the values of hydrogen aromaticity,  $f_{\text{Ha}}$ , obtained using a normal NMR cell agrees well with that obtained for an upside-down cell.

These results indicate that in spite of the fact that the sample was not stirred, the system seems to be homogeneous in the whole of the cell. After the sample was heated up to 833 K, it was then cooled down. The NMR spectrum in the upside-down cell was also observed at room temperature. This implies that dense matter is actually existing in the upper part of the cell.

High-temperature and high-pressure ESR is a useful technique for monitoring the pyrolysis of carbonization reactions. Fig. 5 shows the variation of the radical concentration of CTP as a function of reaction temperature with and without n-paraffin under 10 MPa of nitrogen. For coal-tar pitch alone, the radical concentration shows a marked increase above 673 K. This indicates that an appreciable carbonization reaction of pitch occurs above 673 K. However, during the carbonization of pitch together with n-paraffin, the increase in radical concentration was suppressed and the temperature at which radical concentration increase occurred was shifted to a higher temperature. Paraffin may act as a diluent for pitch.

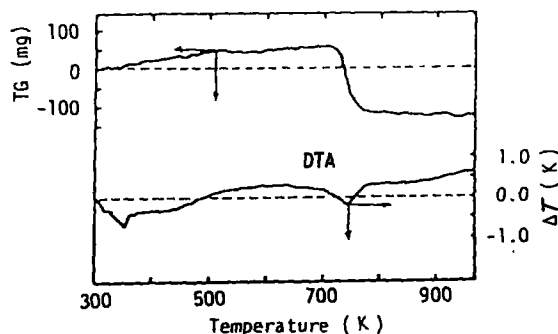


Figure 6 DTA and TG analyses of n-paraffin-pitch (8:2 by weight) system.

\*The  $^1\text{H}$ -NMR spectral line for n-paraffin alone was very sharp at 800 K and no appreciable change of the NMR spectrum was observed from 473 to 723 K, which means that n-paraffin is very stable and does not decompose below this temperature.

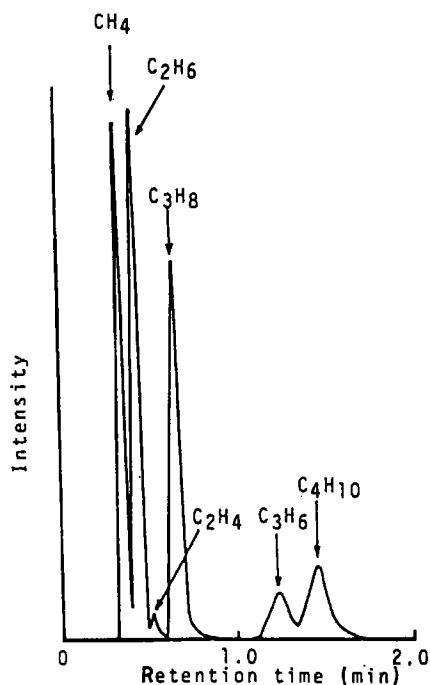


Figure 7 FID gas chromatogram of reaction gas.

Fig. 6 represents DTA and TG curves for the n-paraffin-CTP (8:2 by weight) system. A broad endothermic peak was observed at 743 K and the temperature at which weight decrease was recognized. The decrease in weight started at about 723 K. In the case of pitch alone, no endothermic peak was detected. The endothermic peak observed for the n-paraffin-CTP systems may correspond to the pyrolysis of n-paraffin caused by the pitch carbonization reaction. The final weight loss measured by TG corresponded almost to the weight of n-paraffin.

The threshold temperature for weight decrease coincides with that at which the radical concentration increased markedly in the n-paraffin-CTP (9:1) system, and that at which the NMR signal just appeared using the upside-down cell.

After the carbonization reaction was performed in

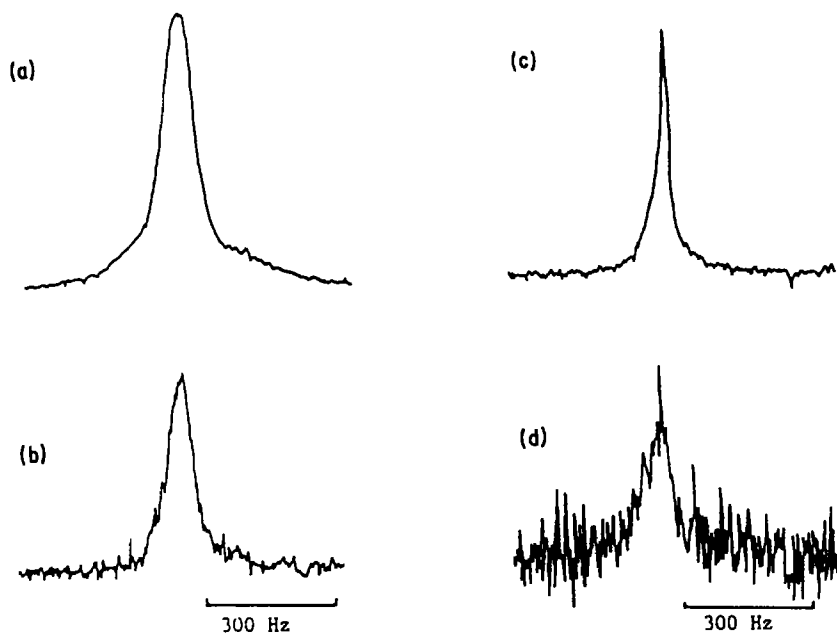


Figure 8  $^1\text{H-NMR}$  spectra of propane at 381 K under (a) 4 MPa, (b) 3 MPa (gain  $\times 4$ ) and those of ethylene at 288 K under (c) 6 MPa, (d) 2.5 MPa (gain  $\times 16$ ).

an autoclave for the mixture of n-paraffin-CTP (8:2) system, the evolved gases were measured by gas chromatography. Fig. 7 shows the gas chromatogram of the reaction gases. The main gases evolved were  $\text{CH}_4$ ,  $\text{C}_2\text{H}_6$  and  $\text{C}_3\text{H}_8$ , while  $\text{C}_2\text{H}_4$ ,  $\text{C}_3\text{H}_6$  and  $\text{C}_4\text{H}_{10}$  were detected as minority gases.

In order to check whether condensed gases gave an appreciable NMR signal or not, we measured the NMR of propane gas at 381 K under 4 MPa. The critical temperature and pressure of propane are 369.8 K and 4.2 MPa, respectively. The observed signal shown in Fig. 8a seems to correspond to condensed gases. The signals are noisy in the conditions below the critical pressure of gases tested, as shown in Fig. 8b.

When the pressure decreases from 4 to 3 MPa, the signal of propane gas becomes weaker. Fig. 8c shows the  $^1\text{H-NMR}$  spectrum of ethylene gas at room temperature under 6 MPa. The critical temperature and pressure of ethylene are 282.9 K and 5 MPa, respectively. With decrease of the pressure from 6 to 2.5 MPa, the NMR signal becomes weaker. From the above results, we can reasonably expect that the observed signal at room temperature for the n-paraffin with CTP system after reaction is in the critical region of some in the mixed gases of  $\text{CH}_4$ ,  $\text{C}_2\text{H}_6$ ,  $\text{C}_3\text{H}_8$  and so on.

By combining the results obtained by these various techniques, a plausible model of carbon microbead formation is sketched in Fig. 9. Initially, n-paraffin and pitch are separate phases (Stage 1). n-Paraffin has poor solubility for solid pitch because the two have different chemical natures. With temperature increase, melted pitch molecules penetrate into the n-paraffin phase by thermal agitation. Pitch takes the form of aggregated microbeads in the continuous phase (Stage 2). The aggregated microbeads separate gradually from each other with increase in temperature. Interfacial tension may be the driving force for them to take a spherical shape. Pyrolysis of n-paraffin occurs with the majority in Stage 3 $^\dagger$ . We have experimented

$^\dagger$ The effect of pyrolysis on bead formation is not yet well understood.

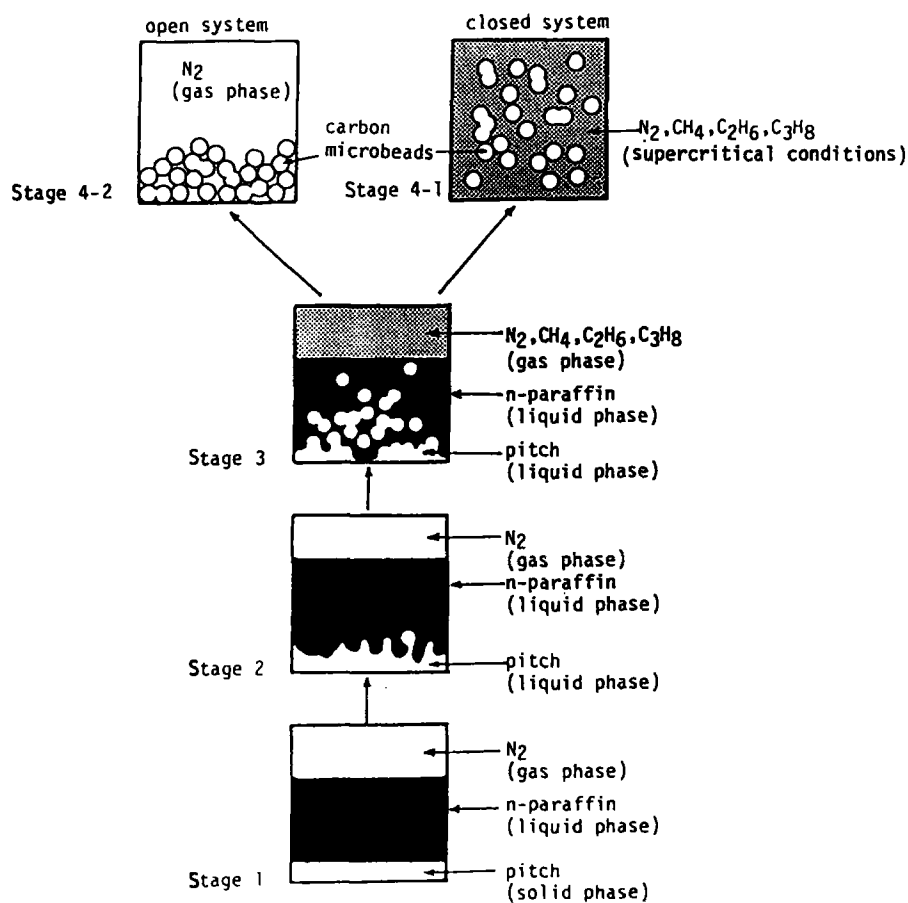


Figure 9 Model of the progressive formation of carbon microbeads. Stage 1:  $T \leq T_m$ . Stage 2:  $T_m \leq T \leq 723 \text{ K}$ . Stage 3:  $723 \text{ K} \leq T \leq 773 \text{ K}$ . Stage 4:  $T \geq 773 \text{ K}$ .

with two further stages, using different sample cells. In the case of the closed cell (Stage 4-1), the pressure of the system increases and it reaches critical gas conditions. The progressive separation of carbon microbeads proceeds under the circumstance of supercritical conditions. This was confirmed by high-temperature and high-pressure <sup>1</sup>H-NMR. On the other hand, in the case of a capillary open cell (Stage 4-2), the thermally evolved gases were allowed to escape from the cell. This was supported by high-temperature and high-pressure TG measurement. Carbon microbead formation was also recognized in the gaseous atmosphere. Differences in the nature of the beads produced under the two conditions are under investigation.

The co-carbonization of n-paraffin with pitch under mild conditions may be a useful method for manufacturing carbon microbeads [7]. A much more favourable method will be expected through a deeper understanding of the mechanism of carbon microbead formation.

## References

1. Y. NAKAGAWA, K. FUJITA and M. MORI, in Proceedings of 17th Biennial Conference on Carbon, Kentucky (American Carbon Society, 1985) p. 409.

2. Y. YAMADA, K. SHIBATA and H. HONDA, *Tanso* **88** (1977) 2.
3. H. HONDA, *Mol. Cryst. Liq. Cryst.* **94** (1983) 97.
4. M. INAGAKI, K. KURODA and M. SAKAI, *High Temp. High Press.* **13** (1981) 207.
5. M. INAGAKI, K. KURODA, N. INOUE and M. SAKAI, *Carbon* **22** (1984) 617.
6. S. SHIMOKAWA, T. YOKONO, J. YAMADA, M. INAGAKI and Y. SANADA, *Carbon* (in press).
7. T. YOKONO, J. YAMADA and Y. SANADA, *J. Mater. Sci. Lett.* **5** (1986) 779.
8. S. SHIMOKAWA, E. YAMADA, T. YOKONO, S. IYAMA and Y. SANADA, *Carbon* **22** (1984) 329.
9. T. YOKONO, S. IYAMA, Y. SANADA, E. YAMADA and S. SHIMOKAWA, Proceedings of Conference on Coal Science (IEA), Sydney, 1985, (Pergamon Press) p. 766.
10. T. YOKONO, S. IYAMA, Y. SANADA and K. MAKINO, *Fuel* **64** (1985) 1014.
11. *Idem*, *Carbon* **22** (1984) 624.
12. T. KOHNO, T. YOKONO, Y. SANADA, K. YAMASHITA, H. HATTORI and K. MAKINO, *J. Appl. Catal.* **22** (1986) 201.
13. K. MAKINO, S. UEDA and S. SHIBAOKA, *Fuel* **57** (1978) 655.

Received 4 March  
and accepted 22 May 1986